CONNEXIN37 PHOSPHORYLATION STATUS DETERMINES DIFFERENT GROWTH PHENOTYPES

By

Ryan Weyker

A Thesis Submitted to the Faculty of the

GRADUATE INTERDISCIPLINARY PROGRAM IN PHYSIOLOGICAL SCIENCES

In Partial Fulfillment of the Requirements

For the Degree of

MASTER OF SCIENCE

In the Graduate College

THE UNIVERSITY OF ARIZONA

2018

STATEMENT BY AUTHOR

The thesis titled ***Connexin37 Phosphorylation Status Determines Different Growth Phenotypes*** prepared by ***Ryan Weyker*** has been submitted in partial fulfillment of requirements for a master's degree at the University of Arizona and is deposited in the University Library to be made available to borrowers under rules of the Library.

Brief quotations from this thesis are allowable without special permission, provided that an accurate acknowledgement of the source is made. Requests for permission for extended quotation from or reproduction of this manuscript in whole or in part may be granted by the head of the major department or the Dean of the Graduate College when in his or her judgment the proposed use of the material is in the interests of scholarship. In all other instances, however, permission must be obtained from the author.

SIGNED: *Ryan Weyker*

APPROVAL BY THESIS DIRECTOR

This thesis has been approved on the date shown below:

Janis M. Burt
Professor of Physiology

Defense Date

6-27-18

Acknowledgements

I would like to thank Tasha Pontifex for her work in creating the stably transfected iRin Cx37-S275,319D and iRin Cx37-S275,328D cell lines and her support on all technical matters molecular and cellular. To Nicole Jacobsen PhD. for her work on the Cx37-WT channels as well as on Cx37-WT 21-Day proliferation assays and Asim Zehri who performed the experiments on the Cx37-S275,319,328D mutant. Lastly, I would like to thank Jose E.K.Viktorin MD. PhD. and John Kanady PhD. for their perpetual patience and wisdom whilst answering my electrophysiology questions.

Contents

Abstract

Cellular growth regulation can be modulated by altering the phosphorylation state of Cx37. Mechanistically it remains to be fully elucidated how Cx37 contributes to this regulation by means of: intramolecular binding partners, its function as a hemi-channel or by facilitation of intercellular communication via gap junctions. Herein we sought to examine the effects of phosphorylation by means of phosphomimetic substitutions (serines to aspartates) on proliferation and the possible alterations to the protein channel function by looking at three mutants Cx37-S275,319D, Cx37-S275,328D and Cx37-S275,319,328D expressed in rat insulinoma cells(Rin). Growth curve assays showed that cells with either Cx37-S275,319D or Cx37-S275,328D eliminated the cell death seen in Cx37-WT and previously studied Cx37 proteins with single site phosphomimetic substitutions at either S275D or S328D, as well as allowing unrestrained proliferation when cells were induced to express the protein at higher densities. Rin cells with Cx37-S275,319,328D appear to proliferate at any density without any measurable cell death. There was a reduction in the open probability for large hemi-channel events for all three non-death inducing mutants and an increased probability of hemi-channels being in the closed state for the growth arrested cells expressing Cx37-S275,319D and Cx37-S275,328D. These data suggest that differential phosphorylation could be an important factor modulating hemi-channel behavior either promoting the closed-state, and thereby facilitating growth arrest and/or preventing high current Cx37 hemi-channel openings and thus facilitating Cx37's capacity to cause cell death.

Introduction

Cellular control of proliferation is fundamental to a healthy organism. One of the regulatory strategies employed by somatic cells to regulate proliferation is the use of connexins to facilitate intercellular communication (*1, 2*). The connexin family is composed of 21 members in humans that all share a similar topology with both a cytoplasmic amino terminus (NT) and carboxyl terminus (CT) along with 4 transmembrane domains connected by 2 extracellular loops and 1 cytoplasmic loop. The distribution and function of connexins are quite varied throughout the body (*3*). In particular the carboxyl terminus provides a great deal of diversity in sequence between connexins with implications for both creating unique channel properties and regulation characteristics (*4, 5*). One of these properties is growth regulation that can result from gap junctional communication(*6*) or with channel independent properties as with the Cx43 CT(*7*).

An excellent model of these growth regulatory effects of Cx expression is the rat insulinoma (Rin) cell which does not express Cx's of any form. However, induced expression of Cx37 specifically, facilitates a diverse phenotype that includes an initial period of cell death and arrest, followed by an extended period of growth arrest and lastly unrestricted growth at rates equivalent to non-expressing cells(*8*). This is paired with a concurrent extension of cell cycle timing during the first 96 hours as seen in serum deprivation studies in Rin cells(*8*). Work done to examine what aspects of Cx37 expression and function are necessary for this growth arrest/extended cell cycle timing to occur suggested that Cx37 must possess its normal pore forming domain sequence(*9*) and an intact carboxyl

terminus(*10*) to enable this regulation. Additionally, our lab has shown that Cx37 must be able to form functional gap junction channels to exert growth suppressive effects in Rin cells(*6*).

It has been shown that connexins, including Cx37(*11*), are phosphoproteins and possess numerous potential phosphosites for regulation by a wide assortment of kinases. We and others have demonstrated the impact phosphorylation can have both pharmacologically with PKC stimulation and inhibition (TPA and BIM, respectively) treatments as well as with dephospho- and phosphomimetic substitutions on the growth phenotype of cells as well as channel electrical properties (*12, 13*). We have created phosphomimetic mutants with serine to aspartate substitutions as well as dephosphomimetic mutants with serine to alanine substitutions at seven consensus serine sites that have a greater than 90% likelihood of being phosphorylated. Results from these substitutions have produced published and unpublished findings that lent themselves to the creation of a model wherein Cx37 functions as a “molecular switch” enabling growth arrest, proliferation and, under certain circumstances, cell death as regulated by phosphorylation status(*12*). In this model, phosphorylation by growth kinases at key sites contributes to channels opening to and between larger conductance states resulting in increased proliferation; however, substitution of all 7 serines to aspartate results in channels preferentially occupying maximal conductance states, which cause cell death(*12*).

Unpublished work by our lab on single site phosphomimetic substitutions as well as a triple S275,319,328D mutation has generated an array of varied phenotypes with some mutations displaying cell-density dependent effects whilst

others seemingly behave without being influenced by cell density. The density-dependence of induced phenotype of several mutants of particular interest to this study are summarized below.

Table 1: Density-dependence of mutant or WT-induced phenotype. Low density environments are defined by cells having minimal cell-cell contact and therefore the hemi-channels(HChs) would be the most probable channel form. Likewise, high density conditions would be where cell-cell contact is widespread and thus there are predominately gap junction channels (GJChs).

	Cell Death (HCh open)	**Growth Arrest (HCh/GJ Closed)**	**Proliferative (Substates)**
WT	Low Density	High/Low Density	High/Low Density
S275D	Low Density	Not seen	High
S319D	Not Seen	High/Low Density	Not Seen
S328D	High/Low Density	Not seen	Not seen

Working with these previously characterized phenotypes we hypothesized outcomes for two double phosphomimetic mutations: S275,319D and S275,328D. For the S275,319D mutant, it was hypothesized that addition of the S319D site to the S275D single mutant would offset the death induced at low density by S275D, revealing an overall phenotype of extended arrest followed by proliferation, as seen Cx37-WT expressing cells. Recognizing that the single S328D mutant protein induces death at both low and high cell density, it was hypothesized that inclusion of two death-inducing sites in the S275,328D mutant would, similarly induce cell death in a density-independent manner. Proliferation studies, serum deprivation experiments, and cell cycle analysis were performed to examine the phenotype of

cells induced to express these double mutants and channel studies were performed to assess the underlying mechanisms.

Here we demonstrate with 21-day proliferation experiments, that neither mutant induced cell death at early time points when cell density is low, unlike the wild-type, and both mutants arrested growth for an extended period before supporting exponential growth towards the end of the proliferation experiment. Serum deprivation experiments showed no cell cycle-stage specific accumulation at high density as well. Study of hemi-channel and gap junction electrical properties to explore a mechanistic basis for these growth characteristics revealed an increased preference for hemi-channels to be in the closed state as well as a trend for 150-280pS amplitude transitions for gap junctions. These results are consistent with our group's molecular switch model of Cx37 function as regulated by phosphorylation status. The presence of density dependent effects on the cell death, cell arrest and cell proliferation phenotypes suggest the need to explore the possible intramolecular interactions of Cx37 and alterations to that might be occurring due to differential phosphorylation status.

Materials and Methods

Cell Culture

All cells were maintained at 37^{o}C at 5% CO in a humidified incubator(*8*). Inducible rat insulinoma (iRin) cells were maintained in RPMI 1640 media (Sigma Aldrich, St. Louis, MO) and supplemented with 10% Fetalplex serum (FP; Gemini Bio Products, West Sacramento, CA). Cellular protein expression was driven by doxycycline via a TET-on system and inducible cells were selected for by inclusion of G418 (300ug/ml; Life Technologies, Grand Island, NY) and hygromycin

(100ug/ml; Life Technologies) in the media. Cells were passed weekly with 0.25% trypsin in divalent-cation-free saline. Doxycycline dosing for maximal protein expression for the different mutants was as follows: 2ug/ml for Cx37-WT, Cx37-S275,319D and Cx37-S275,328D, with 1ug/ml for Cx37-S275,319,328D (S3D).

Mutant Connexin and Expression Vectors

Using the QuikChange site-directed mutagenesis kit (Stratagene, San Diego, CA), the S275,319D / S275,328D / S275,319,328D mutations were introduced sequentially into the pTRE2h-MCx37 plasmid(*8*) using the following oligonucleotide primers (and their respective reverse primers) (Operon Biotechnologies, Huntsville, AL):

S275D Forward: 5' CATGGGCGAGGGACCCTCTGATCCACCGTGTCCCACCTAC 3'

S319D Forward: 5' CAGGGTGGCCGAAAGGATCCTAGCCGCCCCAAC 3'

S328D Forward: 5' CCCAACAGCTCTGCAGACAAGAAGCAGTATG 3'.

Sequences were confirmed by the Genomic Analysis and Technology Core at the University of Arizona.

Proliferation

For 21-day cell counting, cells were plated, as described previously (*8*) at a low density of $3.333x10^4$ cells/cm^2 into 6-well plates. 24 hours after plating cells, 3 wells per plate were induced to start expressing Cx37 protein by treatment with doxycycline (dox+ group), and 3 wells were uninduced (dox-) with no Cx37 protein expression for the entirety of the experiment. All experimental conditions were

run in triplicate, and each experiment was run at least 3 times. At 3-day intervals cells were harvested with trypsin and counted using a Cellometer (Nexcelom, Lawrence, MA). Cell media, with or without doxycycline as appropriate, was refreshed every 2 days. This procedure was modified in the high-density doxycycline swapping experiments to involve induction of previously non-expressing (dox-) wells and removal of doxycycline from Cx37 expressing (dox+) wells at the day 12 time point.

Cells plated for 6-day proliferation monitoring were put at the same $3.333x10^4$ cell/cm^2 density, but into 150mm cell culture dishes. The initial induction (on day 0) with doxycycline occurred 24 hours after plating. Harvesting happened every day using the same procedures as described for the 21-day proliferation monitoring.

Serum Deprivation and Cell Cycle Analysis

1 million cells were plated in 100mm dishes, at an approximate density of 12,739 cells/cm^2, in the presence of serum. 24 hours later cells were either retained in 10% Fetalplex serum (“Serum+”) or swapped into a serum-starved condition (0% serum, “serum-“) for 48 hours. After this point cells were induced with doxycycline (hour -24) and allowed to express for 24 hours before harvesting began. Harvesting was done (starting at the 0 hour time point), by trypsinizing cells and resuspending in 10ml of media before being counted with a cellometer (Nexcelom, Lawrence, MA). Additionally, non-adherent cells were collected and counted when refreshing cell media at hours 0 and 48. All harvested cells were spun down into a pellet and then resuspended in 70% ethanol whilst being

vigorously vortexed and were then stored at -20^{o}C for up to 2 weeks. After repelleting, the ethanol was aspirated and the cells resuspended in cold 1xPBS at a density of 1x10^{6} cells/ml. 500ul of each sample was aliquotted into 3ml snapcap tubes containing a solution of 50ug RNase A and 100ug/ml of propidium iodide. Samples were incubated for 30 minutes at 37^{0}C before undergoing FACS analysis.

Electrophysiology

In order to evaluate HCh and GJCh behavior, cells were plated at low densities, to acquire both isolated single cells as well as isolated cell pairs, on glass coverslips and doxycycline added to induce expression. For HCh activity, cells were dosed 48hrs in advance of recording to achieve maximal protein expression. Assessment of GJChs was done within 24hrs of dox induction, to increase the likelihood of finding cell pairs with low conductance values <1nS. Recordings were done by placing a glass coverslip into a custom-made chamber and bathing cells in an external solution composed of: 142.5 mM NaCl, 4 mM KCl, 1 mM $MgCl_2$, 5 mM glucose, 2 mM Na Pyruvate, 10 mM HEPES, 15 mM CsCl, 10 mM TEA-Cl, 1 mM $CaCl_2$, pH adjusted to 7.2 (315 mOsM). Patch pipets (2-15 MΩ) contained: 124 mM KCl, 14 mM CsCl, 9 mM HEPES, 9 mM EGTA, 0.5 mM $CaCl_2$, 5 mM glucose, 9 mM TEA-Cl, 3 mM $MgCl_2$, 5 mM Na_2ATP, pH 7.2, 315 mOsM. Rhodamine dextran was added to at a final concentration of 10μg/ml in the internal solution for GJCh recordings.

HCh Electrophysiology

Cells were prepared and examined as previously described(*8*), using whole-cell voltage-clamp techniques with Axopatch 1-C amplifiers and pClamp software (Molecular Devices, Sunnyvale, CA). Assessment of HCh open probability (Po) was done by making recordings of cells given a 30 s pre-pulse at +25mV and a subsequent ~240 s of pulsing at +25mV, before, in-between and after these pulses were 10 seconds of 0mV holding potential. Seal integrity and cell viability was monitored before and after experiments. Recordings were filtered, decimated and divided into 0.25pA bins ranging from -2.5pA to +40pA with the frequency of each bin being calculated individually. These values were plotted as a percent frequency against current. The 0pA "closed state" during the +25mV pulse was identified on the current frequency plots by either visual inspection or peak fitting with Origin software. For the purposes of statistical analysis and in keeping with previous work (*12*) we consolidated data from these 0.25pA bins into ranges representing channel states, -2.5-+2.5pA "closed state", +2.5pA-+7.5pA "low-current sub-state", +7.5pA-+12.5pA "high-current sub-state", +12.5pA-+20pA "fully open", +20pA-40pA "multiple open channels". These consolidated bins were assessed for differences across Cx37 isoforms using 1-way ANOVA and Tukey's multiple comparisons test using Prism software.

Gap Junction Transitions

Cells were prepared and examined in a manner similar to the HChs, but with dual-whole-cell voltage clamp. Cell pairs were assessed for bridges either with visual inspection for a failure of rhodamine-labeled dextran (Molecular Probes, Eugene, OR) to label both cells as it cannot permeate the gap junction(*14*)

or by looking for less than 1nS of conductance tested with +10mV pulses. Cell pairs that did have less than 1nS of conductance were subjected to experiments to record single channel transition events. Cell pairs were subjected to alternating ±10mV pulses in intervals of 5 s with equal length pauses at 0mV before going to a +25mV for the portion of the record to be assessed. Subsequently returning to the alternating ±10mV pulses to confirm seal integrity.

Transitions were measured where current levels were stable for at least 50ms pre and post-transition. All current values were transform into conductance values (pA/25mV) for analysis and reporting purposes. Similar binning was done for the transitions as for Po assessment with appropriate scaling for GJChs such that 0-50pS was considered a low amplitude transition, 50-150pS and 150-250pS were intermediate transition amplitudes and 250-400pS as large transition amplitudes. Statistical differences were then assessed between different isoforms for the various conductance groupings using 1-way ANOVA and Tukey's multiple comparisons test using Prism software.

Statistics

Statistical comparisons of 21-day cell count monitor experiments (including swapping experiments) and 6-day proliferation monitoring were done with unpaired t-tests using Holm-Sidak method for multiple comparisons. Serum deprivation experiments were analyzed with 2-way ANOVA with a Tukey's post hoc test. Electrophysiological data was compared as described above with use of 1-way ANOVA's with Tukey's post hoc test. Significant differences were determined by a $P<0.05$. Error bars represent mean ±S.E.M.

Results

Phenotypic consequences of Cx37-S275, 319D and Cx37-S275,328D expression

Cx37-WT is growth suppressive at low and high cell density. Previous, as yet unpublished work from our lab, showed that Cx37-S275D induces cell death at low, but not high cell density whereas Cx37-S319D does not induce death at any density, instead inducing growth arrest in a density independent manner. With these single site mutant characteristics in mind we hypothesized that the S319D mutation might protect against the death induced by S275D at low cell density and support proliferation after an arrested growth period.

To test this hypothesis, we first assessed proliferation over a 21-day period. Cells were plated at low density and cell number monitored with continuous induction of expression with doxycycline. Cx37-S275,319D expression in Rin cells resulted in an extended 12-day period of growth arrest, similar to the 12-15 days seen with WT (**Fig. 1A**). After this period of growth arrest both WT and the S275,319D mutant supported uninhibited proliferation.

In contrast to the density dependent induction of cell death by Cx37-S275D, previous studies (unpublished) also demonstrated that Cx37-S328D induces cell death at all cell densities. Thus, we hypothesized that the double Cx37-S275,328D mutation would induce death at all cell densities. To test this hypothesis, we first performed 21-day proliferation studies. In contrast to expectations we found that much like the Cx37-S275,319D mutant, Cx37-S275,328D expression induces an extended period of growth arrest, no cell death, and transitioning to proliferation, possibly at an earlier time point than WT (**Fig. 1B**).

Phenotypes for both mutants display density dependence.

Since Cx37-S275D induced cell death at low plating density, but supported proliferation at higher plating density, we next evaluated both double mutants for density-dependent phenotypic effects. There was no evidence of an early period of cell death at the low plating density used in the 21-day proliferation assays presented above (**Fig. 1A,B**, insets). We examined this early period with greater resolution in 6-day proliferation assays sampling cell number daily rather than every three days. In these assays, cells were plated at the same low density as in the 21-day assays, $3.33x10^3$ cells/cm^2, but in larger plates thereby increasing counting accuracy. The data show that both double-site mutants are not significantly different from the WT (**Fig. 2A**) and present with arrested growth, but not cell death at this low density.

To determine whether the prolonged growth arrest period induced by Cx37-S275,319D and Cx37-S275,328D in cells at low-density were evident at high density, doxycycline swapping experiments were undertaken. Cells were grown in the absence of Cx37 expression, for 12 days followed by 9 days of expression controlled by the absence and presence of doxycycline respectively. For Cx37-S275,319D, cell density increased from $3.33x10^3$ cells/cm^2 (at day 0) to $1.37x10^5$ cells/cm^2 (at day 12) before protein expression with doxycycline induction began, and cell density continued to increase after doxycycline induction with no obvious growth inhibition compared to the untreated control (**Fig. 2B**). A similar outcome was observed for Cx37-S275,328D cells, with cell density increasing from $3.33x10^3$ cells/cm^2 (at day 0) to $1.18x10^5$ cells/cm^2 (at day 12) before induction occurred for the last 9 days of the experiment. Like Cx37-S275,319D there is no inhibition of growth as compared to untreated controls (**Fig. 2C**).

Phenotypic consequences of Cx37-S275,319D and Cx37-S275,328D on cell cycle.

To ascertain in which phase of the cell cycle the double mutants were arresting, we used FACS with propidium iodide staining. Cells were plated in the presence of serum for 24h and either kept in serum or switched to serum free medium for 48h, at which point doxycycline was added. 24h after addition of doxycycline (time 0 on graphs) and every 24h thereafter, cells were harvested and cell cycle analysis performed. Contrary to expectation, in the presence of serum the cells were not growth arrested (**Fig. 3A,B**) and had a similar percentage of cells in G_1/G_0 at start (0hrs) as they did at the end (+96hrs). The cell proliferation observed in these experiments suggests the experimental design was not ideal given the density dependent effects of these mutants. In other words, at the time of doxycycline induction (-24 hours), the cells were likely already at a density where both mutants support proliferation (similar to the **Fig. 2A,B** experiments). The densities reached at -24hr time point in the case of Cx37-S275,319D is around 17,707 cells/cm^2 and 22,292 cells/cm^2 for Cx37-S275,328D are ~5-6.5 fold higher than for those seen at the start of 21-day proliferation experiments. Thus, it remains to be determined in what phase of the cell cycle these mutants arrest proliferation when cells are at low density.

As mentioned above, Cx37-S275D and Cx37-S328D induced cell death, which was readily detected in FACS experiments by the presence of a "sub-G_1 peak" (cells with less than a full complement of DNA) in the presence of serum (data not shown). Neither the Cx37-S275,319D nor CX37-S275,328D mutants induced detectable cell death, as evident from the lack of a sub-G_1 peak (**Fig. 3C,D: black arrows)**. Thus, the data support that these double phosphomimetic substitutions protect against the cell death that the single site mutations induce.

Taken together these data suggest that both Cx37-S275,319D and Cx37-S275,328D expressing cells possess two phenotypes at low density (growth arrest and proliferation) and a single phenotype at high density (proliferative). It is intriguing that expression of Cx37-S275D induces death of cells plated at low-density and Cx37-S328D induces death of cells at all densities, whereas the double mutant expressing cells are rescued by the inclusion of a single additional phosphomimetic site, even when those single sites, mutated individually, induce death.

S275,319D,328D (S3D) has only a growth permissive phenotype.

In previous studies done in our lab the phenotypic consequences of expressing the triple mutant wherein all three serine residues targeted in our double mutants, serines 275, 319 and 328, were replaced with aspartate (Cx37-S3D). 21-day proliferation assays revealed that this mutant supported proliferation throughout the assay period (**Fig. 4A and inset**); proliferation was not different from non-induced WT or S3D expressing cells. Cell cycle analysis showed that G_1/G_0 accumulation occurred when cells were serum starved and not proliferating, however, no such accumulation occurred when the cells were proliferating in the presence of serum(**Fig. 4B**). This difference in cell cycle progression and proliferation also occurred in the absence of induced cell death (**Fig. 4C**). Thus, substitution of these three phosphomimetic sites appears sufficient to alleviate the cell death induced by WT and growth arrest induced by both WT and the double mutants while in the presence of serum.

S275,319D and S275,328D Hemi-channels(HChs) share similar properties.

In previous studies, Jacobsen et al, 2017 suggested that differential hemi-channel (HCh) vs. gap junction channel (GJCh) function dictated, at least in part, the differential effects of Cx37 (mutants) at low (where HCh form, but GJCh don't form due to lack of cell-cell contact) vs. high plating density (where both HCh and GJCh can form and function). Specifically, mutations that caused the HCh to favor the fully open state were proposed to cause cell death at both low and high cell density, HCh and GJChs that favored the closed state were proposed to induce cell cycle arrest, and HCh and GJCh that preferred the sub-state conductance values were suggested to favor cellular proliferation. With this framework in mind, we assessed the behavior of the HChs formed by the double mutants. Cells were voltage clamped at +25mV for the duration of the open probability assessment period, bracketed by 0mV time points to verify membrane and voltage clamp integrity. Compared to WT expressing cells, the closed state probability (determined as current values between -2.5 and +2.5 pA) was significantly increased for S275,319D HChs (**Fig. 5A, see adjacent difference plots for visualization**). In addition, there was a significant decrease in the probability of the mutant channel fully opening (current values between 12.5 and 20 pA) and a decrease in the likelihood of more than one hemi-channel being open during the recording (>20pA) (**Fig. 5A**). This result is consistent with our previously proposed model (*12*).

It was important to validate the possibility of an increased closed state probability in Cx37-S275,328D cells given the very similar growth phenotype to Cx37-S275,319D cells. The data suggest that the closed state probability of for Cx37-S275,328D HChs is comparable to the Cx37-S275,319D HChs (**Fig. 5B)**. A

direct comparison of the two double-site mutants was undertaken to see if they possessed any important distinctions in HCh properties. Subsequent to that, the only significant difference is found at the low-current sub-state (defined as channel opening in the range of 2.5-7.5pA), but they are otherwise not significantly different from each other (**Fig. 5C)**. The overall characteristics for both channels are similar.

Cx37-S3D Hemi-channels characteristics.

As Cx37-S3D is a mutant that grows without any period of growth arrest at low density, we evaluated the HChs formed by this mutant for their preferred open state. In comparison with wild type the S3D mutant displays a decreased likelihood of opening fully, particularly above 15pA, and a decreased likelihood of multiple channels being active at any given time pA>20 (**Fig. 6A**). This is particularly important given our previous work on the S7D mutant, which dies at any density and, like the WT, is both more likely to open fully and to have more than one hemi-channel open at once (*12*). This characteristic appears to set death-inducing mutants apart from those that are merely growth arrested, or like the S3D, grow without issue. A further comparison of the S3D mutant, this time to the growth arrested double site mutants, reveals a greater preference for single channels to not be in the closed state and to open more frequently to various sub-states for the channels. (**Fig.6B**). Thus, the evidence supports the idea that mutations that limit the open probability of fully open HChs are less likely to suffer cell death.

Impact of mutants on gap junction transitions.

It had been shown previously in our lab that expression of Cx37-WT at high densities (where the vast majority of cells are expected to be physically touching each other), in experiments similar to those shown in **Fig. 2B,C**, that cells become growth arrested and proliferation ceases. The apparent difference in phenotype of cells expressing WT compared to those of Cx37-S275,319D, Cx37-S275,328D, and Cx37-S3D suggested to us that there might be differences in how the gap junctions are functioning. Therefore we undertook electrophysiologic recordings of coupled cells to examine transitions for individual channels. Each of the mutants trend towards favoring transitions of intermediate amplitude compared to WT as shown by their individual difference plots (WT-isoform). This intermediate range for Cx37-S275,319D varies between ~180-240pS (**Fig.7A**) and for Cx37-S275,328D between ~130-200pS (**Fig.7B**). The intermediate range for Cx37-S3D varied between ~210-300pS (**Fig.7C**). Without dwell time data, these transition amplitude data are difficult to interpret. However, if it is assumed that GJCh open probability preferences are well predicted by HCh behavior, then these data are consistent with double mutant GJChs preferring the closed state, but transitioning to and from this intermediate state to the closed state. Together these data indicate a likely difference for these mutants from Cx37-WT that merits a more in-depth examination of GJCh open probabilities.

Discussion

The ability of Cx37 to regulate the growth phenotype of Rin cells was first established in 2008 (*8*). Since that time it has been demonstrated that growth phenotype regulation by Cx37 requires the entire CT of Cx37 (*10*), an intact Cx37-

comprised pore forming domain (*9*), and the ability to form functional gap junction channels (*6*). The CT of most connexins contains numerous potential phosphorylation targets that could differentially regulate the protein's contribution to cell functions in diverse ways such as modifying affinity for intra- and inter-molecular partners(*15*), enhancing Cx assembly and/or degradation (*16*), and altering gap junction and/or hemi-channel properties(*17*).

In our present work we sought to address how phosphorylation, in various combinations, at serines 275, 319 and 328 affected the growth phenotypes induced by Cx37 in Rin cells. Our lab and others have established a role for phosphorylation of connexins in regulating proliferation (*12, 18, 19*). In particular, the S275 site, which is a predicted target of MAPK8, presents as a potential key residue in such regulation. A key role for this residue in modulating Cx37's regulatory effects is suggested by density dependent effects of expressing Cx37-S275D: death vs. proliferation at low vs. high density, respectively. We show that addition of aspartate substitutions at either S319 or S328 to Cx37-S275D rescues cells from death at low-density. This rescue from death at low density, is associated with a reduced preference of the HCh for the fully open state and increased preference for the closed state. This increased closed state preference is in concurrence with previous work suggesting that HChs that are more likely to be closed promote a growth arrested phenotype. The HChs formed by the density-independent growth permissive Cx37-S3D do not favor the closed state but also do not favor the fully open state, consistent with previous studies suggesting fully open HChs induce cell death while closed channels favor growth arrest (*12*). Additionally, trends of the gap junctions for each mutant towards intermediate amplitude transitions present the possibility of a particular GJCh

profile conducive to proliferation, however, it will be important to establish the open probability for each mutant to help more clearly reveal what characteristics are necessary for a Cx37 gap junction to enable proliferation.

That closed HChs favor a growth arrested state suggests that either a reduction in transmembrane signaling or altered protein-protein interactions with intracellular growth regulatory proteins may be the mechanism underlying Cx37-mediated growth arrest. Previous work from other labs has shown association of Cx37 with eNOS(*20*), MAPK/ERK proteins, and the cell cycle regulator P27 (*21*), therefore it will be important to continue examination of the interactome of Cx37 to identify “non-channel” roles for Cx37 that are critical to understanding its full role as a regulator of proliferation.

In summary, our work demonstrates the importance of differential Cx37 phosphorylation in regulating growth phenotype of Rin cells as demonstrated by phosphomimetic substitutions. Although these serine to aspartate substitutions have limitations, such as differences in size or loss of dynamic regulation at the phosphosite as compared to adding/removing a phosphate group, they are still powerful tools to explore the impact of phosphorylation. Overall, the S275 site presents as a possible lynchpin of Cx37 regulation by MAPK8 activity whereby cells are enabled to grow at high density when gap junctions are expected to dominate. Additionally, as the phosphorylation profile of Cx37 changes, there appears to be different HCh channel opening profiles, some of which are able to limit the potentially deleterious large/multi-channel HCh openings. It will be important to follow up with studies of paired aspartate substitutions at S319 and S328 in order to isolate clearly the role of the S275D site.

Figure Legends

Figure 1. **Cx37-S275,319D and Cx37-S275,328D show similar growth arrest phenotypes and trend towards faster growth than wild-type.** (A) 21-day proliferation monitoring of Cx37-S275,319D (N=5) expressing Rin cells plated at an initial density of 3,333 cells/cm^2 in 6-well plates run in triplicate shows no strong indication of cell death at any time points and unrestricted growth starting around day 15. (B) Cx37-S275,328D (N=5) expressing cells show a similar lack of a death phenotype with growth arrest appearing to cease around day 15 with a trend towards faster proliferation than the WT (N=6). Red and blue asterisks indicate differences ($p<0.05$) between mutant ±dox conditions while black asterisks are differences between mutant dox+ and WT dox+ ($p<0.05$). *Insets*: Expanded Y-axis plot of each respective proliferation graph.

Figure 2. **Cx37-S275,319D and Cx37-S275,328D possess similar phenotypes at both low and high density.** (A) Cells were plated at the same low density as those in **Fig 1,** at 3,333 cells/cm^2, but into 150mm dishes, which allows for greater accuracy in cell counting. Cells expressing either double mutant Cx37 isoform showed no differences from Cx37-WT expressing cells in proliferation at this low density (N=3). (B) Cells were divided into four groups, all plated at 3,333 cells/cm^2 density into 6-well plates, these groups were those who were in either dox+ or dox- conditions for the entire 21 days (red lines) or those who were swapped at day 12 either into or out of the dox+ condition (dox-,+ and dox +,- respectively, gold lines). Experiments were performed 3 times with each dox condition run in triplicate for all time points, for Cx37-S275,319D there was no significant difference for groups grown in the absence of doxycycline (dox-) and those induced to express protein at day 12 (dox-,+). This indicates an inability for Cx37-

S275,319D to growth arrest Rin cells. (C) For Cx37-S275,328D three experiments were run with the same dosing groups as described in (B) and likewise there was also a lack of significant differences between the Dox- and Dox -,+ groups indicating a lack of growth arrest at high density seen previously for WT (data not shown). *Insets*: Expanded Y-axis plot of each respective proliferation graph.

Figure 3. **Rin cells expressing Cx37-S275,319D and Cx37-S275,328D are not growth arrested in the presence of serum and show evidence of ameliorated cell death.** (A) Cells were plated into 100mm dishes at a density of 12,738 cells/cm^2 in the presence of serum (10% fetalplex). After 24 hours the "serum-" group was swapped into a 0% serum starved condition and both groups received doxycycline induction at the "-24hr" time point. Cells expressing Cx37-S275,319D showed a difference in proliferation at the +72 and +96 hour time points between the serum conditions (green asterisks $p<0.05$), however, there was a distinct lack of G_0/G_1 accumulation for either group as assessed by propidium iodide staining followed by FACS (N=3). The serum+ groups unrestricted growth is suggestive that the plating density for the experiment may have been too high to see growth arrest. (B) Rin cells expressing Cx37-S275,328D were subjected to the same procedures described in (A) (N=3). In a similar fashion, Cx37-S275,328D have an appearance of unrestricted growth in serum+ conditions as compared to the serum- at the +72hr and +96hr time point. (green asterisks, $p<0.05$). Additionally, there is no indication of G_0/G_1 accumulation in either serum condition. (C) Representative images were selected showing the PI labeling at the +96hr time point for both double mutants. There was no major presence of cell debris, an indicator of a less than full complement of DNA and thus dead or dying cells. This is contrasted with previous experiments on the single site mutants Cx37-S275D

and Cx37-S328D which had large accumulations of debris suggesting an amelioration of the death induction for those single site mutants.

Figure 4. **Cx37-S3D shows unrestricted growth in the presence of serum, growth arrest in 0% serum with G_0/G_1 accumulation and no indication of cell death.** (A) 21-day proliferation assays, performed as previous described in Fig 1a, showed no significant differences between the proliferation of Rin cells either induced (dox+) or not induced (dox-) into expressing Cx37-S3D. This indicates a total relief of all growth arresting affects as seen in Rin cells expressing the WT Cx37 (dox+) (N=4). (B) Serum deprivation experiments, performed as previous described in Fig 2a, showed uninhibited growth in serum+ conditions, but growth arrest for the serum starved cells (green asterisks, proliferation serum+ vs. serum-, $p<0.05$). This is paired with an increase in G_0/G_1 accumulation suggesting cells are arresting in that phase of the cell cycle. (C) The proliferation of the Cx37-S3D cells is concurrent with an absence in cell death, indicated by a lack of cell debris (see black arrow).

Figure 5. **Cx37-S275,319D and Cx37-S275,328D HChs show a similar preference for being closed as well as avoiding the full open state.** (A) Cx37-S275,319D HChs were measured by pulsing cells at +25mV for ~240s and binned into .25pA sections of recording with an open probability(Po) calculated for each of these bins (N=6). These values were plotted on the graph as open probability as a function of current values as well as a difference plot subtracting the Po's of Cx37-S275,319D from WT. Bins were consolidated into ranges constituting the "closed state" -2.5pA to +2.5pA, "low-current sub-state" 2.5pA-7.5pA, "high-current sub-state" 7.5pA-12.5pA, "fully open state" 12.5pA-20pA, and "multiple channel

openings" 20pA-40pA. A comparison of these ranges via 1-Way ANOVA with Tukey's post hoc indicated Cx37-S275,319D HChs are preferentially found more commonly in the closed state than WT HChs. Cx37-S275,319D HChs also appear to avoid the fully open state as well as not having multiple channels open at the same time in contrast to the WT($p<0.05$). (B) Cx37-S275,328D HChs (N=12) also show an increase in the closed state and avoidance of the channel fully opening or having multiple channels open at the same time($p<0.05$). (C) A comparison of the two double mutants suggests a strong similarity in HCh profile with the only major difference being Cx37-S275,328D having a tendency to open more frequently at the 2.5pA-7.5pA low-current sub-state($p<0.05$).

Figure 6. **Cx37-S3D HChs close as often as WT, but shows reduced Po for fully open/multiple channel openings in a manner similar to Cx37-S275,319D and Cx37-S275,328D.** (A) Examination of Cx37-S3D HCh Po behavior (N=5) showed no difference from the WT in how often channels are in the closed state ($p<0.05$), but there was a reduction in how often Cx37-S3D HChs opened fully or had more than one channel open at a time as compared to WT. (B) This avoidance of these large current events was found to be similar when looking at Cx37-S3D vs. Cx37-S275,319D and Cx37-S275,328D HChs. Cx37-S3D does have an increased Po for the sub-states compared to either double mutant suggesting a possible way that Cx37-S3D expression in Rin cells can promote growth at any density.

Figure 7. **Cx37 mutants show a trend towards increased prevalence of intermediate amplitude transitions for GJChs.** Cell pairs shown to linked by gap junctions, confirmed by means of either rhodamine dextran labeling of just one of the cells (gap junctions are impermeable to the dye) or low coupling (<1 nS

conductance) were assessed. The cell pairs with gap junctions found to be under 1nS of conductance were provided with ~5s pulses alternately applied to the cells one at a time with ±10mV pulses interspersed between 0mV pulses to establish a baseline. One side of the pair would then be subjected to a +25mV pulse and the opposing cell recorded from for assessment of transitions before reapplying the alternating ±10mV to confirm seal integrity. Cx37-S275,319D GJCh transitions (N=3) were measured as current values and transformed in conductance values (pA/mV) in 10pS bins plotted as a relative frequency. These data when compared to the WT suggest a trend for a preference towards intermediate transitions in the range of ~180-240pS. (B) Cx37-S275,328D GJChs (N=3) as visualized in the difference plot seem to prefer transitions around ~130pS-200pS. (C) For Cx37-S3D GJChs (N=4) the preferred transitions appear to be grouped in the ~210pS-300pS range.

Figures

Figure 1

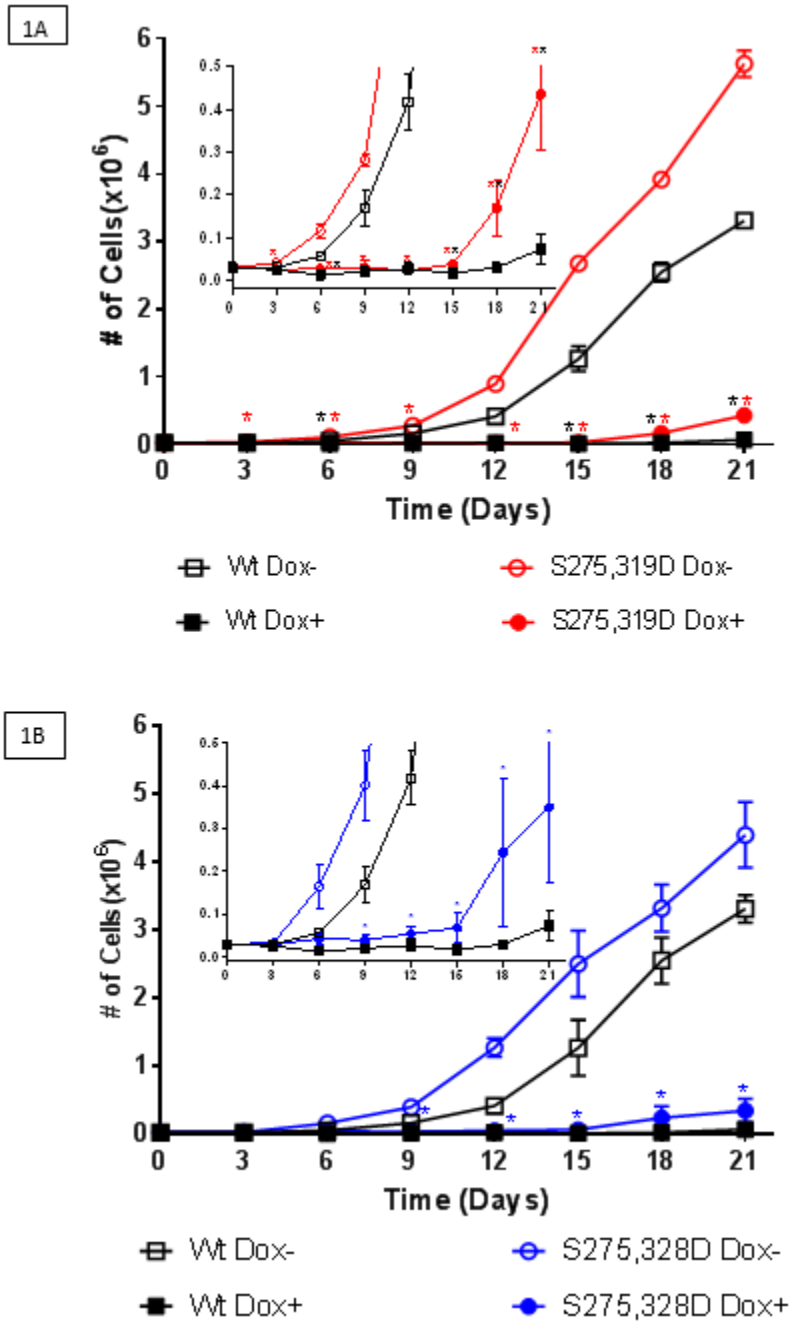

Figure 2

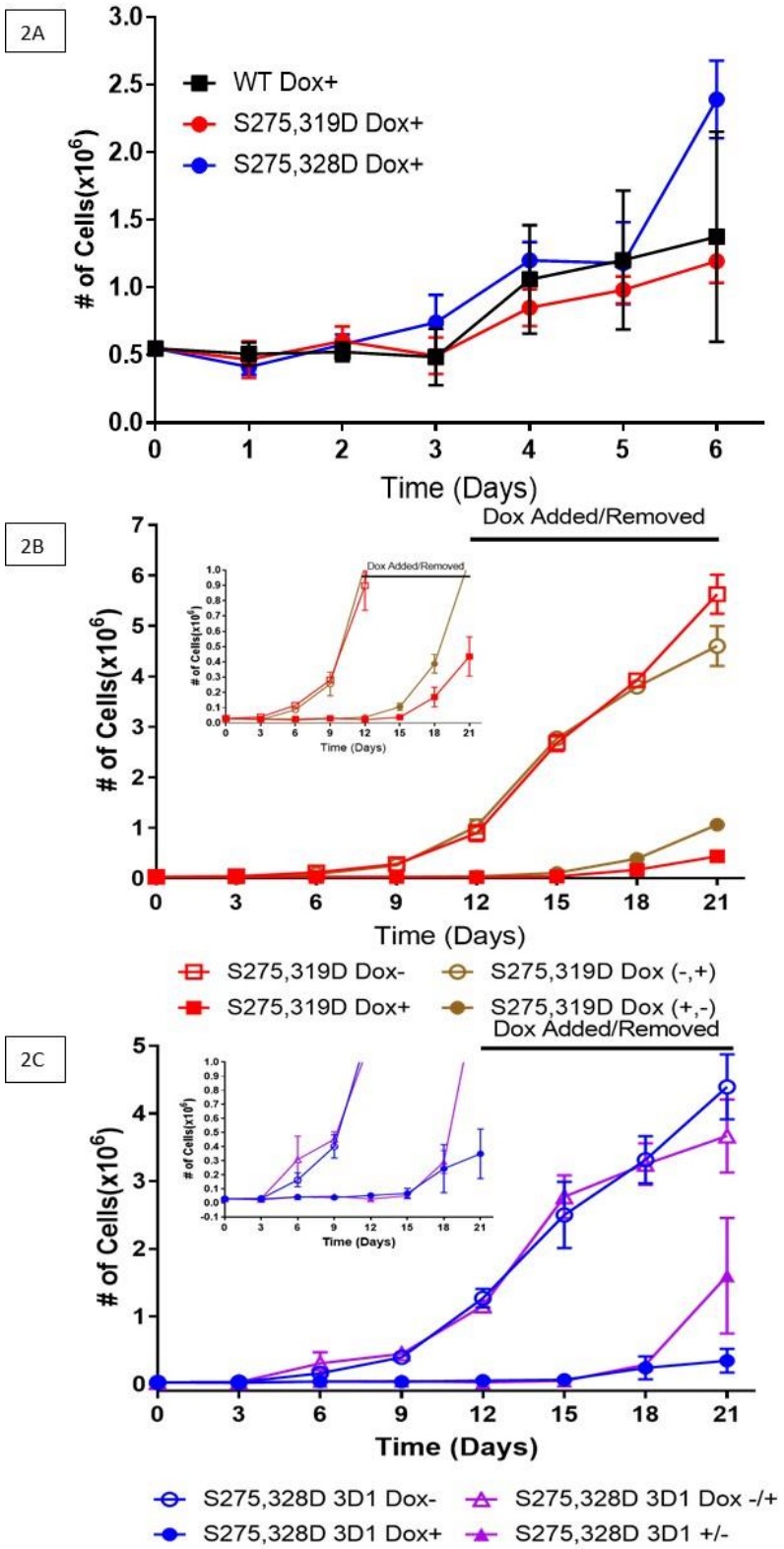
2A
WT Dox+
S275,319D Dox+
S275,328D Dox+
# of Cells(x10^6)
Time (Days)
2B
Dox Added/Removed
# of Cells(x10^6)
Time (Days)
S275,319D Dox-
S275,319D Dox+
S275,319D Dox (-,+)
S275,319D Dox (+,-)
2C
Dox Added/Removed
# of Cells(x10^6)
Time (Days)
S275,328D 3D1 Dox-
S275,328D 3D1 Dox+
S275,328D 3D1 Dox -/+
S275,328D 3D1 +/-

Figure 3

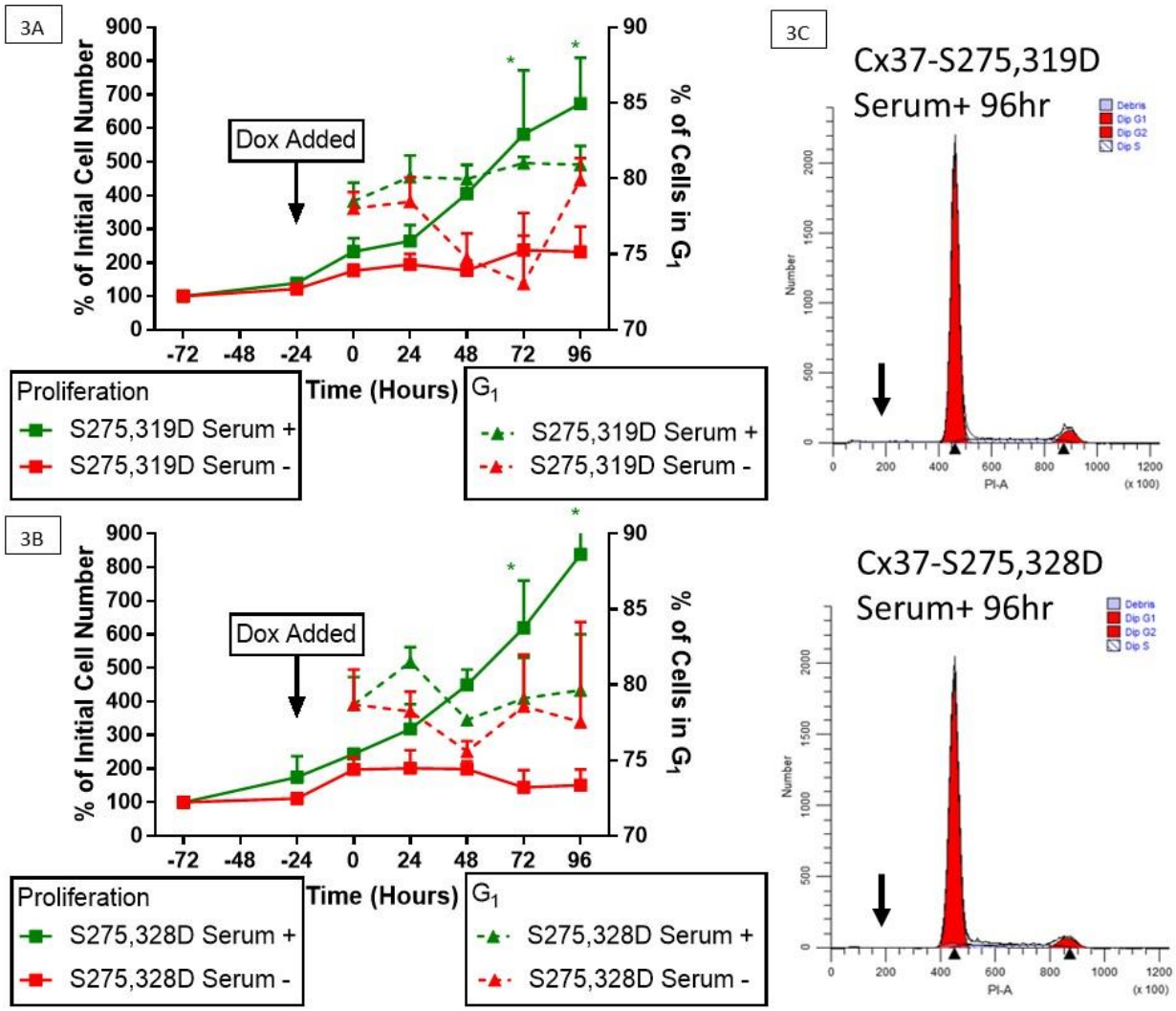
3A
% of Initial Cell Number
% of Cells in G1
Dox Added
Time (Hours)
Proliferation
S275,319D Serum +
S275,319D Serum -
G1
S275,319D Serum +
S275,319D Serum -
3B
% of Initial Cell Number
% of Cells in G1
Dox Added
Time (Hours)
Proliferation
S275,328D Serum +
S275,328D Serum -
G1
S275,328D Serum +
S275,328D Serum -
3C
Cx37-S275,319D
Serum+ 96hr
Debris
Dip G1
Dip G2
Dip S
Number
PI-A
(x 100)
Cx37-S275,328D
Serum+ 96hr
Debris
Dip G1
Dip G2
Dip S
Number
PI-A
(x 100)

Figure 4

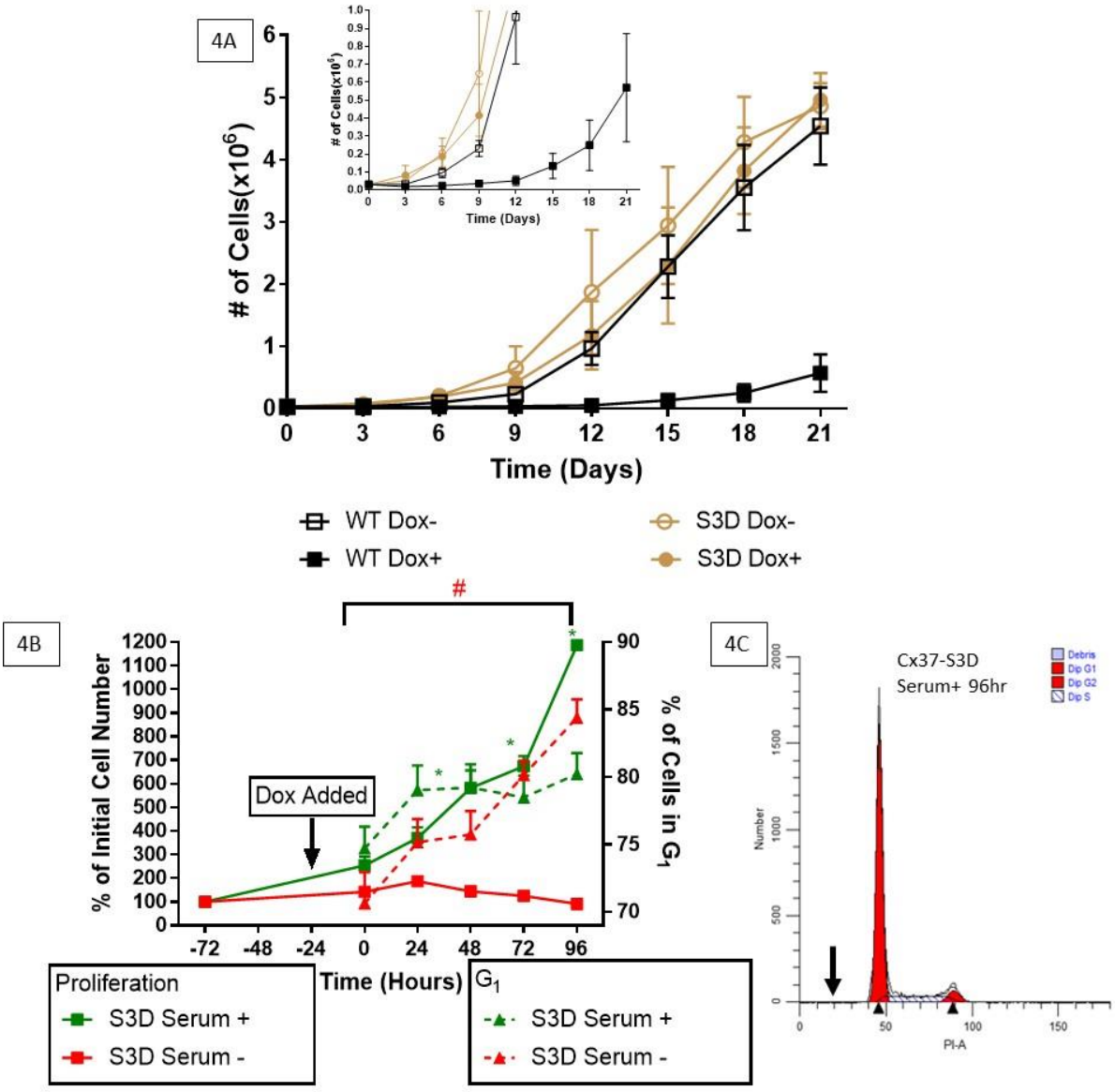
4A
# of Cells(x10^6)
Time (Days)
WT Dox-
WT Dox+
S3D Dox-
S3D Dox+
4B
% of Initial Cell Number
% of Cells in G1
Dox Added
Time (Hours)
Proliferation
S3D Serum +
S3D Serum -
G1
S3D Serum +
S3D Serum -
4C
Cx37-S3D
Serum+ 96hr
Debris
Dip G1
Dip G2
Dip S
Number
PI-A

Figure 5

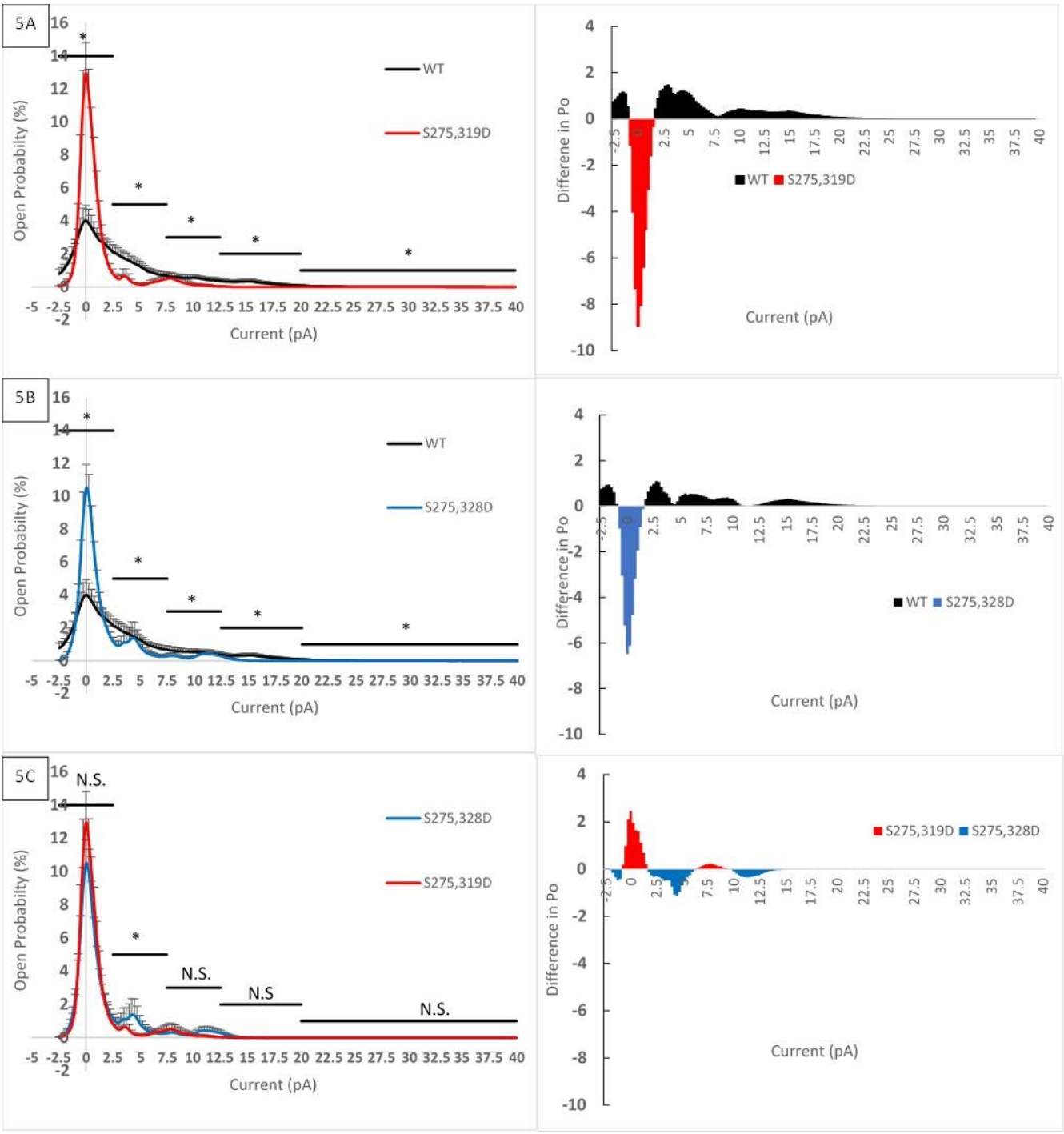
5A
Open Probability (%)
Current (pA)
WT
S275,319D
*
Differene in Po
Current (pA)
WT S275,319D
5B
Open Probability (%)
Current (pA)
WT
S275,328D
*
Difference in Po
Current (pA)
WT S275,328D
5C
N.S.
Open Probability (%)
Current (pA)
S275,328D
S275,319D
*
N.S.
N.S
N.S.
Difference in Po
Current (pA)
S275,319D S275,328D

Figure 6

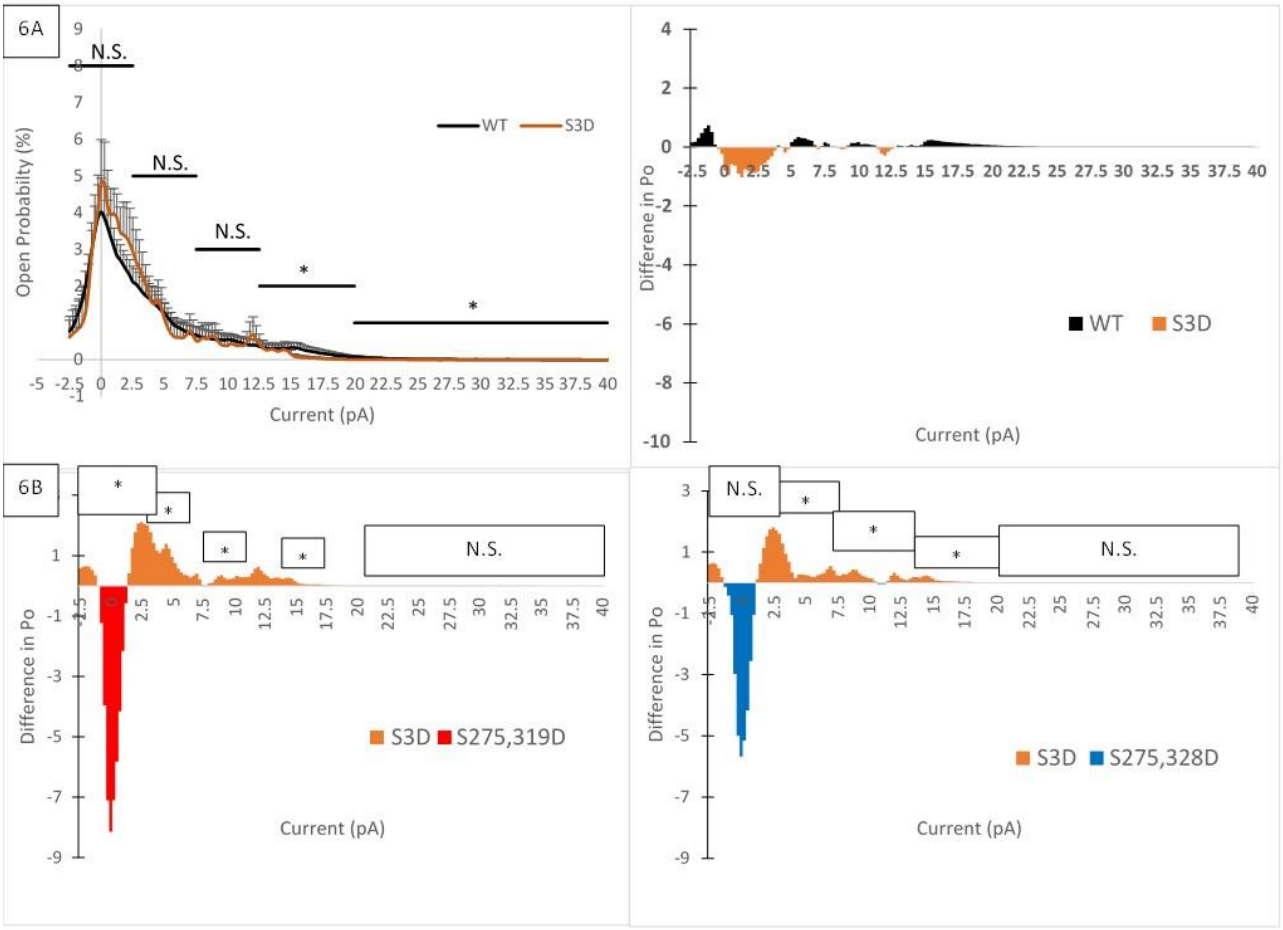
6A
N.S.
N.S.
N.S.
*
*
WT
S3D
Open Probability (%)
Current (pA)
Differene in Po
WT
S3D
Current (pA)
6B
*
*
*
*
N.S.
Difference in Po
S3D
S275,319D
Current (pA)
N.S.
*
*
*
N.S.
Difference in Po
S3D
S275,328D
Current (pA)

Figure 7

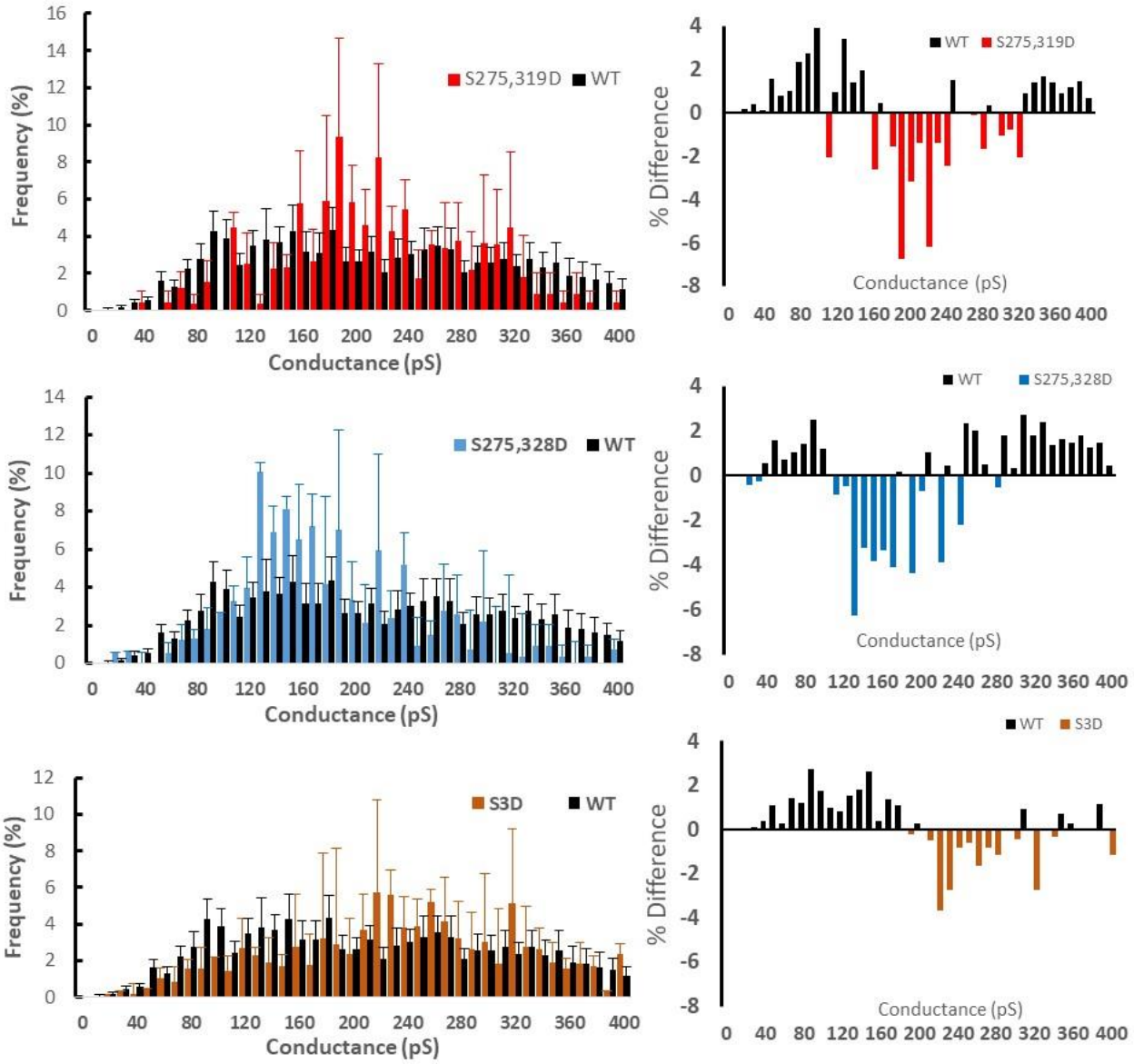
Frequency (%)
S275,319D
WT
Conductance (pS)
% Difference
WT
S275,319D
Conductance (pS)
Frequency (%)
S275,328D
WT
Conductance (pS)
% Difference
WT
S275,328D
Conductance (pS)
Frequency (%)
S3D
WT
Conductance (pS)
% Difference
WT
S3D
Conductance (pS)

References

1. W. R. Loewenstein, Y. Kanno, Intercellular communication and the control of tissue growth: lack of communication between cancer cells. *Nature* **209**, 1248-1249 (1966).
2. W. R. Loewenstein, Junctional intercellular communication and the control of growth. *Biochim. Biophys. Acta* **560**, 1-65 (1979).
3. G. Sohl, K. Willecke, Gap junctions and the connexin protein family. *Cardiovasc. Res* **62**, 228-232 (2004).
4. J. L. Solan, P. D. Lampe, Connexin phosphorylation as a regulatory event linked to gap junction channel assembly. *Biochim. Biophys. Acta* **1711**, 154-163 (2005).
5. J. F. Ek-Vitorin, J. M. Burt, Structural basis for the selective permeability of channels made of communicating junction proteins. *Biochim. Biophys. Acta* **1828**, 51-68 (2013).
6. M. E. Good, J. F. Ek Vitorin, J. M. Burt, Structural determinants and proliferative consequences of connexin 37 hemichannel function in insulinoma cells. *J. Biol. Chem* **289**, 30379-30386 (2014).
7. X. Dang, B. W. Doble, E. Kardami, The carboxy-tail of connexin-43 localizes to the nucleus and inhibits cell growth. *Mol. Cell Biochem* **242**, 35-38 (2003).
8. J. M. Burt, T. K. Nelson, A. M. Simon, J. S. Fang, Connexin 37 profoundly slows cell cycle progression in rat insulinoma cells. *Am. J. Physiol Cell Physiol* **295**, C1103-C1112 (2008).
9. M. E. Good, T. K. Nelson, A. M. Simon, J. M. Burt, A functional channel is necessary for growth suppression by Cx37. *J. Cell Sci* **124**, 2448-2456 (2011).
10. T. K. Nelson, P. L. Sorgen, J. M. Burt, Carboxy terminus and pore-forming domain properties specific to Cx37 are necessary for Cx37-mediated suppression of insulinoma cell proliferation. *Am. J. Physiol Cell Physiol* **305**, C1246-C1256 (2013).
11. D. M. Larson *et al.*, Functional expression and biochemical characterization of an epitope-tagged connexin37. *Mol. Cell Biol. Res. Commun* **3**, 115-121 (2000).
12. N. L. Jacobsen *et al.*, Regulation of Cx37 channel and growth-suppressive properties by phosphorylation. *J. Cell Sci.* **130**, 3308-3321 (2017).
13. K. Pogoda *et al.*, NO Augments Endothelial Reactivity by Reducing Myoendothelial Calcium Signal Spreading: A Novel Role for Cx37 (Connexin 37) and the Protein Tyrosine Phosphatase SHP-2. *Arterioscler. Thromb. Vasc. Biol.* **37**, 2280-2290 (2017).
14. J. F. Ek-Vitorin, J. M. Burt, Quantification of Gap Junction Selectivity. *Am. J. Physiol Cell Physiol* **289**, C1535-C1546 (2005).
15. C. Ambrosi *et al.*, Connexin43 Forms Supramolecular Complexes through Non-Overlapping Binding Sites for Drebrin, Tubulin, and ZO-1. *PLoS One* **11**, e0157073 (2016).
16. H. Li, G. Spagnol, L. Zheng, K. L. Stauch, P. L. Sorgen, Regulation of Connexin43 Function and Expression by Tyrosine Kinase 2. *J. Biol. Chem.* **291**, 15867-15880 (2016).
17. N. Batra *et al.*, Direct Regulation of Osteocytic Connexin 43 Hemichannels through AKT Kinase Activated by Mechanical Stimulation. *J. Biol. Chem* **289**, 10582-10591 (2014).
18. S. R. Johnstone *et al.*, MAPK phosphorylation of connexin 43 promotes binding of cyclin E and smooth muscle cell proliferation. *Circ. Res* **111**, 201-211 (2012).
19. S. Morel *et al.*, Unexpected role for the human Cx37 C1019T polymorphism in tumour cell proliferation. *Carcinogenesis* **31**, 1922-1931 (2010).
20. A. Pfenniger *et al.*, Gap junction protein Cx37 interacts with endothelial nitric oxide synthase in endothelial cells. *Arterioscler. Thromb. Vasc. Biol* **30**, 827-834 (2010).
21. J. S. Fang *et al.*, Shear-induced Notch-Cx37-p27 axis arrests endothelial cell cycle to enable arterial specification. *Nature communications* **8**, 2149 (2017).